NUKLEONIKA 2011;56(2):107–112

ORIGINAL PAPER

Diagnostics and scaling of fusion-produced neutrons in PF experiments

Hellmut Schmidt

Abstract. Neutrons from a plasma focus (PF) device operated in a deuterium gas, measured as a function of time, location and direction of emission, reveal quite a number of important parameters on fusion reactions occurring in the dense high-current phase of the experiment. In addition the determination of the energy spectra of the emitted neutrons is important for understanding the mechanisms taking place for the neutron production. Results of neutron measurements in large experiments such as the former POSEIDON experiment in Stuttgart and the PF-1000 experiment in Warsaw are presented. The neutron diagnostic methods that had been utilized include nuclear track detectors, plastic scintillators coupled to photomultipliers, activation measurements, time-of-flight methods as well as pinholes for spatial resolution of the neutron source. The well known scaling law according to which the neutron yield scales roughly as the square of the energy input or the fourth power of the current is discussed. Reasons for strong deviation from this law for high energies – known as the saturation effect – are still a subject of debate.

Key words: neutron emission • plasma focus • scaling laws • neutron diagnostics • nuclear fusion

H. Schmidt
International Centre for Dense Magnetized Plasmas,
23 Hery Str., 01-497 Warsaw, Poland
and Institut für Plasmaforschung,
Universität Stuttgart,
Pfaffenwaldring 31, 70569 Stuttgart, Germany,
Tel.: 0049 7032 22156, Fax: 0049 7032 921 919,
E-mail: mail@hellmutschmidt.de

Received: 30 August 2010
Accepted: 15 October 2010

Introduction

The research and development effort related to PF devices was started nearly half a century ago in Russia [3] and USA [15], and later also in Europe [14,17], Asia [10] and Africa as well. Large plasma focus devices were operated among others at the Kurchatov Institute, Moscow, Russia (since 1962), the Lebedev Institute, Moscow, Russia (since 1968), at Los Alamos, USA (since 1964), at CEA Limeil in France (1968–1979), in Frascati, Italy (1970–1982), and at the Institut für Plasmaforschung (IPF) in Stuttgart, Germany (1970–1995). In 1997 the International Centre for Dense Magnetized Plasmas (ICDMP) was established in Warsaw, Poland, and the Fusion Laboratory has recently been founded in Australia [11]. Although many questions regarding the efficient operation of PF devices for fast ion, fast electron, X-ray and neutron emission had been solved, there remains still a lot to be done to properly understand and control processes taking place, especially at the beginning and the end of a discharge. The variation in the proportion of neutrons produced in thermonuclear reactions and beam-target interaction and their scaling with the input energy are still a subject of investigation. This paper concentrates on the neutron emission of PF devices. In particular, results on the detection of time-integrated and time-resolved fusion-produced (fast) neutrons using activation methods, nuclear track detectors,

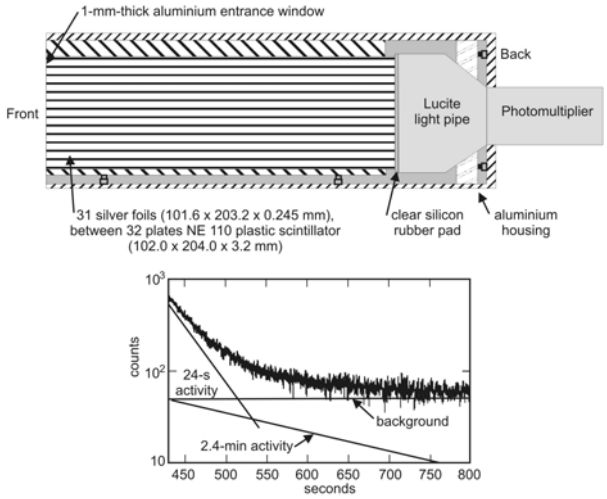

Fig. 1. An example of a specific design for a silver activation counter. When used with fast neutrons, the counter is normally placed within a polyethylene moderator. The plot shows the counting rate observed for a period from 450 to 800 s following the exposure to a fast neutron flux.

scintillation/photomultiplier detectors and thermoluminescent dosimeters (TLDs) are reported. Neutron diagnostic methods used in the experiment include the time-of-flight spectroscopy and neutron pinholes with time-resolved detection. It is concluded that a dominant mechanism of the neutron production is of beam-target type of an interaction between fast electromagnetically accelerated deuterons and the compressed dense plasma. The so-called gyrating particle model (GPM) is invoked to explain the experimental results.

The analysis of the fusion reaction kinetics leads us to the conclusion that neutron diagnostics should be supplemented with proton diagnostics, realized by assessing the tracks etched in nuclear track detectors.

Finally the scaling of the neutron yield as a function of the pinch current and the input energy is presented, and saturation effects are discussed.

Neutron detection

The most common method to detect neutrons without time resolution is by activation of suitable materials. Many laboratories rely on the activation of silver combined with e.g. plastic scintillators and photomultipliers (see Fig. 1) or more often with proportional counters. As most materials show high activation cross sections for slow neutrons [13] (see Table 1), fast neutrons have to be moderated before detection. This leads then to the problem of sensitivity to the scattered neutrons. In some laboratories the Be activation method is used to avoid or minimize the contribution of scattered neutrons [13] (see Fig. 2). Be-based counters have in addition the advantage of a short (807 ms) half-time. Therefore they are useful for detection of neutrons in devices with repetition rates of up to about 1 Hz.

There is a plan by ICDMP to compare the Be counters from laboratories in Singapore, USA and Poland using the PF-1000 device being operated in Warsaw [8, 23] as the neutron source. This would then allow for a more reliable comparison of the neutron yields of various devices operated in different labs.

Table 1. Comparison of various elements employed for pulsed neutron detection

Element	Half-life $\tau_{1/2}$ (s)	Reaction	Neutron energy	Operation mode	Particle detected	Reference
Arsenic	0.017	$^{75}As(n,n')^{75m}As$	Fast	Reperitive	γ	[10]
Beryllium	0.807	$^{9}Be(n,\alpha)^{6}He$	Fast	Reperitive	β	[12]
Boron trifluoride	…	$^{9}B(n,\alpha)^{7}Li$	Thermal	Reperitive	α	[13]
Helium-3	…	$^{6}He(n,p)^{3}H$	Thermal	Reperitive	p	[14]
Indium	14.1	$^{115}In(n,\gamma)^{116}In$	Thermal	Single	β	[6]
Rhodium	42.3	$^{103}Rh(n,\gamma)^{104}Rh$	Thermal	Single	β	[11]
Silver	24.6 142	$^{109}Ag(n,\gamma)^{110}Ag$ $^{107}Ag(n,\gamma)^{118}Ag$	Thermal	Single	β	[9]

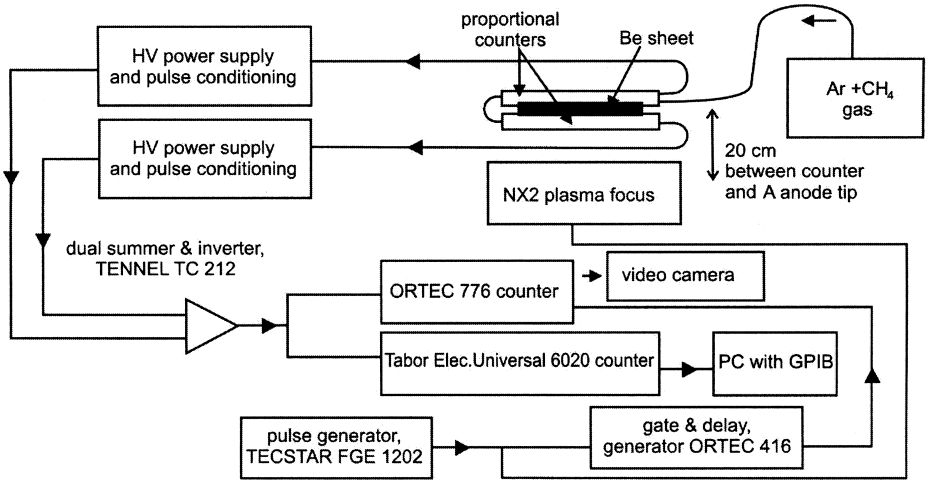

Fig. 2. A schematic diagram of the beryllium counter, used at NX2 plasma focus, with the triggering system and the data acquisition system.

To determine the time-integrated anisotropy of the neutron emission in the PF-1000 device [7] TLDs together with Bonner spheres were used.

For time-resolved neutron detection in various directions (to determine the anisotropy) and at various distances (to determine the spectral distribution), plastic scintillators with photomultipliers had been mainly used. In recent experiments scintillators with decay times in the sub-nanosecond region were used together with ultrafast photomultipliers [23]. If signals can be recorded with multi-GHz oscilloscopes, the temporal characteristics of the neutron emission may be determined in a much more precise way than several years ago.

Neutron diagnostic methods

The appearance of two consecutive neutron pulses correlated with the pinch dynamics was observed for the first time in POSEIDON [19]. It was possible to measure the anisotropy and the spectral distribution of these neutron pulses and also the dynamic spatial evolution of such pulses using a neutron pinhole with several scintillation detectors in the detection plane [20]. There are plans to repeat these measurements also for the PF-1000 device.

The anisotropic emission (in the axial and the radial directions, respectively) of the two neutron pulses mentioned above is shown in Fig. 3.

For high neutron yield the anisotropy of the first neutron pulse is smaller than unity, whereas for the second pulse the anisotropy is larger than unity. The higher the neutron yield in a shot, the larger is the anisotropy.

Measurements performed using a neutron pinhole and seven scintillator/photomultiplier detectors in the detection plane, corresponding to 2 cm separation in the axial direction of the POSEIDON PF (resolution is limited to about 1 cm), allowed to determine the axial movement of the neutron emitting region. Neutron signals registered in a single shot are shown in Fig. 4. Neutron pinhole measurements were previously performed using the Frascati Megajoule PF [14].

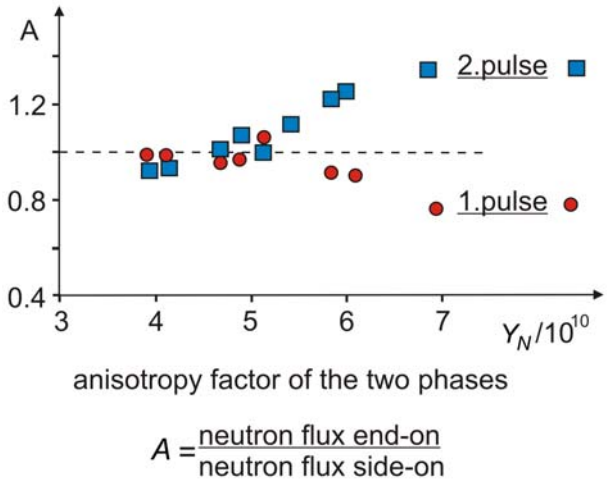

Fig. 3. An anisotropy A of the neutron fluence for the two neutron pulses, as a function of the total neutron yield Y_N for shots with filling under the pressure of 8 hPa and the input energy of 280 kJ at 60 kV.

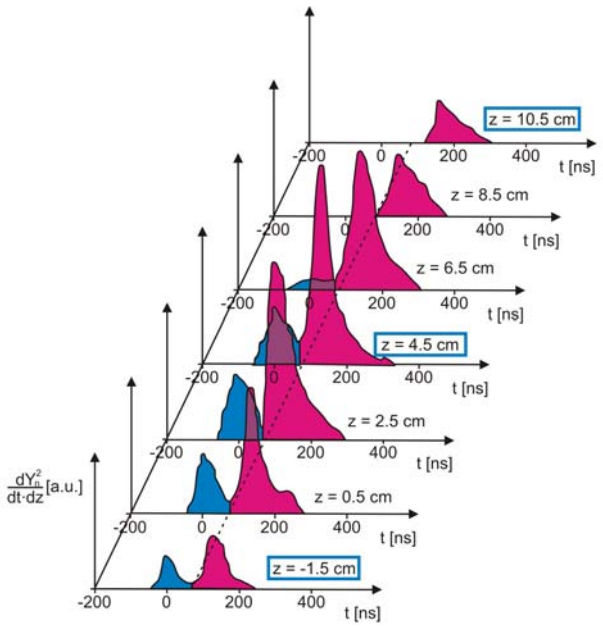

Fig. 4. Results of neutron pinhole measurements performed in a single shot. Time- and space-resolved emission from various areas ($\Delta z = 2$ cm) along the axis may be seen. Temporal resolution of 20–30 ns had been achieved. The first pulse extends only to $z = 6.5$ cm. The second pulse is shifted some 40 ns in time from $z = 0$ to $z = 10$ cm.

When detectors are located at various distances from the neutron source, as was done in the case of POSEIDON in the radial direction, i.e. perpendicular to the electrode axis, the time resolved neutron spectra may be extracted from the registered signals. In Fig. 5 a typical spectrum for the primary and secondary neutron pulse is presented using (a) equal-density-lines and (b) the integrated signal. Subtle time correlations between the registered signals have to be taken into account. This is facilitated by the fact that X-ray signals are also registered by the detectors. The scattering of neutrons must be accounted for and its effect on the measurement should be minimized. As described in

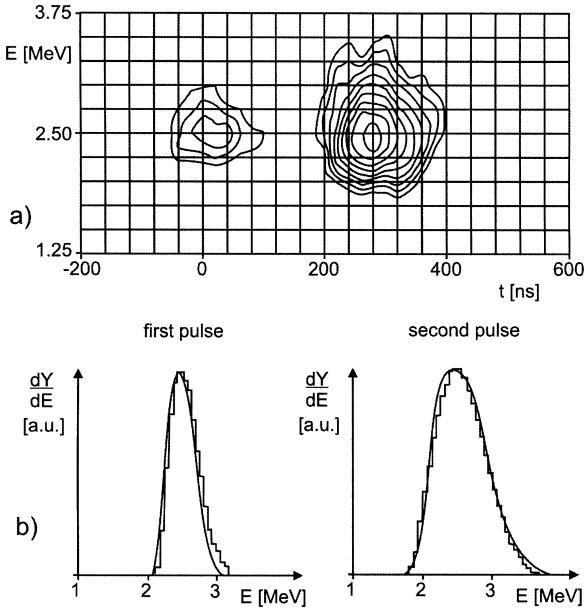

Fig. 5. A reconstruction of the neutron spectrum of a typical POSEIDON shot (no. 7522), at 8 hPa and 380 kJ at 70 kV.

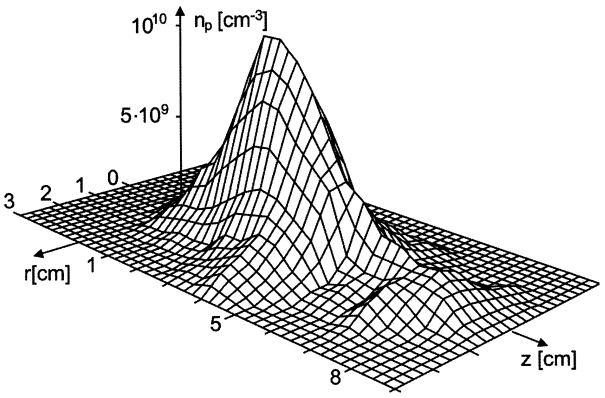

Fig. 6. Three-dimensional (3D) reconstruction (using a modified Abel-inversion method) of a proton pinhole picture from the shot 6561 at POSEIDON, at 5 hPa and 280 kJ at 60 kV. The source extends approximately 9 cm in the axial direction and 6 cm in the radial direction.

a paper by Schmidt R *et al*. [22], there exists an optimum positioning of the locations of the detectors.

Proton diagnostics

The dd-reaction occurs with equal probability in two channels, one producing neutrons (2.45 MeV) and the other one protons (3.02 MeV). Proton measurements could therefore be used as a complement to the neutron measurements [5]. Protons have the advantage that e.g. in the pinhole measurements a much higher resolution may be achieved than in the neutron pinhole measurements. On the other hand, they have the disadvantage of being deflected by magnetic fields, especially in the vicinity of the pinch. An example of a proton pinhole image is shown in Fig. 6.

Fusion reaction kinetics in plasma neutron sources GPM

As mentioned above, the information on the energy and directional distributions of fast deuterons may be obtained only in an indirect way. In Ref. [5] it was assumed that fast deuterons gyrate in pinch structures. The model is called a gyrating particle model (GPM). The directional distribution of the deuterons after electromagnetic acceleration is usually anisotropic. The anisotropic emission may be described using the anisotropy factor n_d, $n_d = 2\ln A_d/\ln 2$, where $A_d = f$(end-on)$/f$ (side-on).

For the simulation of the measured neutron or proton emission, the following assumptions were made [5]:

1. For the distribution function of fast deuterons, a quasi temperature T_i^* was assumed.
2. The deuteron sources were assumed to be point sources localized on the axis. With deuteron energies ranging in the interval 20 keV < E_d < 500 keV, the measured neutron and proton spectra could be satisfactorily described for POSEIDON by taking into account various magnetic field distributions for the two neutron emission phases. A schematic cross section of the POSEIDON plasma, at the time of the first neutron pulse, is shown in Fig. 7. Figure 8 shows the trajectories of 18 monoenergetic deuterons, emitted at $(r, z) = (0,0)$ under various angles to the axis [5]. For lower energies the helical trajectories would be smaller in diameter and would lie closer to the axis. The pinch current for the simulations was assumed to be 800 kA in the axial direction.

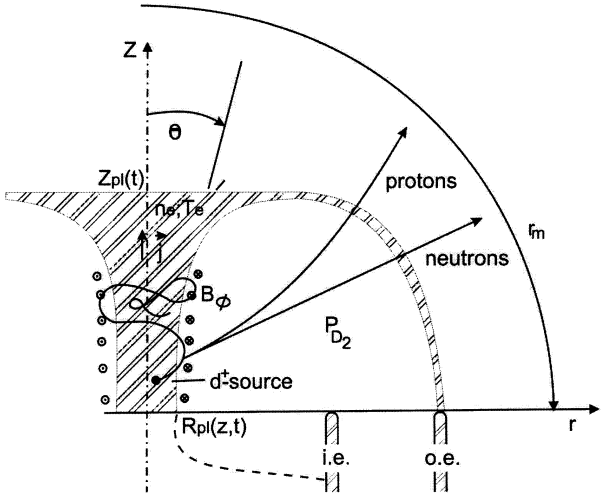

Fig. 7. The geometry of the POSEIDON PF in a quiet phase at $t = 0$ (maximum compression). A spiralling deuterium trajectory for $Ip = 0.8$ MA, $n_e = 8 \times 10^{18}$ cm^{-3}, and $T_e = 0.6$ keV is shown. The diameter of the inner electrode is 131 mm. Early on the path, a fusion collision is shown leading to emission of a neutron or a proton, respectively.

Thermal or beam-target neutrons?

Neutron and beam diagnostics have revealed that in the PF and Z-pinch experiments the measured neutron emission is predominantly caused by beam-target processes occurring between high-energy deuterons and

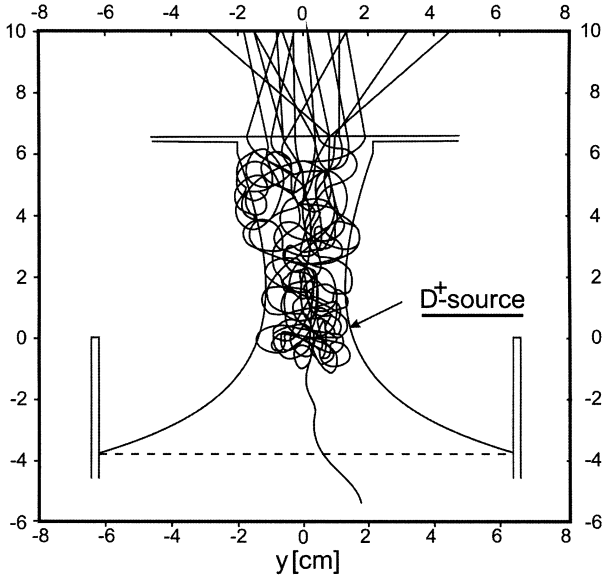

Fig. 8. Trajectories of 18 monoenergetic deuterons emitted in the angular range of 0° < Θ < 180° with energy of 140 kV in the quiet phase. A pointlike deuteron source is located at $r = 0$, $z = 0$. The plasma dynamics and the deuteron energy relaxation are both accounted for. The deuteron motion is terminated when E_d < 2 keV.

the dense pinch plasma. There are at least five strong indications for this process:

1. The generation of high energy ions (tens of keV to several MeV) was found e.g. from interferometric measurements [2]. The so-called bubble propagates into the initially neutral gas in front of the anode. The interferometrically measured electron [2] or spectroscopically measured ion [6] density wave propagates with high velocity. Detection of fast ions is also reported in this workshop [9].
2. The measured anisotropy in the neutron emission [21] can only be explained by the contribution of beam target processes and not by the neutron production in a thermal plasma. Anisotropy factors smaller than unity (see Fig. 3) may be explained by assuming that fast ions move primarily in the radial direction.
3. The time-of-flight neutron measurements reveal in the downstream (upstream) direction neutrons with energies much higher (lower) than the 2.45 MeV reaction energy.
4. A detailed time-dependent neutron spectroscopy (by time-of-flight measurements) indicates relaxation effects on the deuteron energy during the two neutron emission phases identified in POSEIDON (see Fig. 9).
5. Estimates of thermally produced neutrons, taking into account density, temperature, volume and the lifetime of the pinched plasma, result in contributions which are only a few percent of the measured neutron yield.

A detailed discussion of neutron production processes in large Z-pinch devices [24] favours thermal neutron production, which up to now has not been supported by the experimental data. One has to admit, however, that with increasing current, temperature and density the percentage contribution of thermal neutron production might increase considerably, as has been shown in simulations [18]. In that paper it was concluded, that – assuming a constant beam production efficiency – in the case of a breakeven pinch device, the contribution of beam target processes to the fusion energy would range between 10 and 30%. It was also concluded that in a PF device or a Z-pinch with radial magnetic confinement, where no additional heating is applied, the contribution of beam target processes to the energy balance of a fusion reactor reduces the initial energy input requirements, but thermal fusion energy production strongly dominates, especially for small axial dimensions.

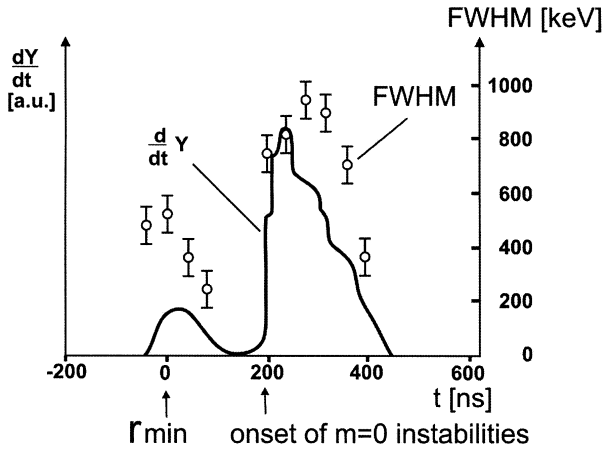

Fig. 9. Full width at half maximum (FWHM) of neutron spectra for a POSEIDON shot at 8 hPa and 380 kJ; for the primary pulse we have $Y_N = 6 \times 10^9$, and for the secondary pulse $Y_N = 4.1 \times 10^{10}$. The neutron spectral width is initially increasing, but then decreases for the primary pulse as well as for the secondary pulse, indicating the slowing down of the fast deuteron component.

Scaling of neutron yield and saturation

Neutron yield of optimized PF devices or Z-pinches increases roughly as the 4th power of the discharge current or the square of the input energy (usually stored in capacitors). In 1977 Bernard [2] included low-energy Z-pinches in a plot of the neutron yield as a function of the discharge current (see Fig. 10). The Darmstadt group [16] reported for their small device about 50 times higher yield than expected on the basis of scaling. In a comparison of experiments [4], the saturation of the neutron yield was reported for two large devices (POSEIDON in Stuttgart and PF-360 in Świerk), showing also the dependence on the choice of the material for the insulators. PF devices with ceramic insulators seemed to give higher yield than e.g. those with glass insulators.

There are several effects which might be responsible for the saturation behaviour:

1. Sub-optimal plasma engineering, i.e. deficiencies in the breakdown during the initial phase and/or in the current and density sheath formation.
2. Deficiencies in establishing anomalous resistivity during the compression phase.
3. Influence of inadequate impurity content.
4. Inadequate decoupling of the initial and final phases due to static gas filling.

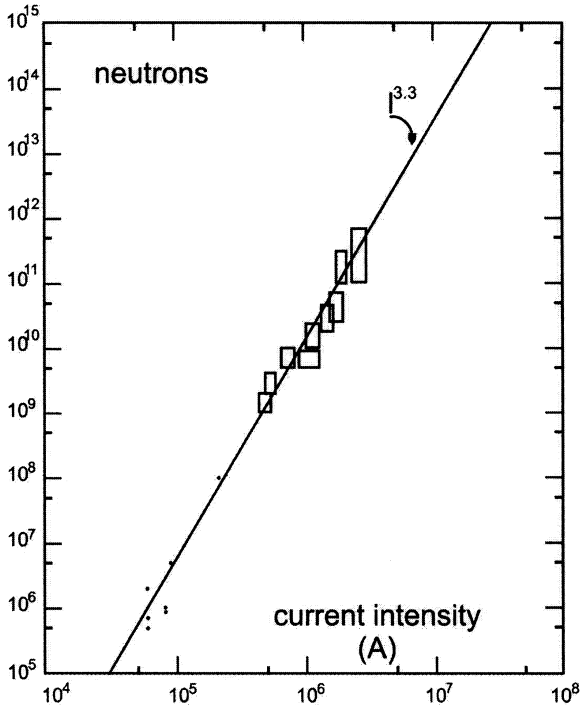

Fig. 10. The neutron scaling as a function of the current intensity of various PF and Z-pinch experiments.

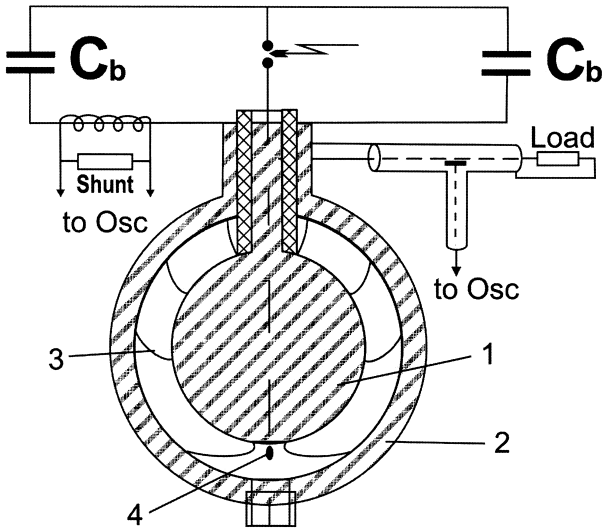

Fig. 11. A spherical plasma focus: C_b – condenser bank; 1 – anode; 2 – cathode; 3 – plasma sheath position in time; 4 – zone of PF formation.

It is strongly suspected that the general effect of saturation of neutron yield with increasing input energy cannot be explained by recent simulations [12] with conventional simple cylindrical electrode geometry. Other geometries (see Fig. 11) should also be taken into consideration [1]. Even in the devices with a conventional design, e.g. POSEIDON, a sudden decrease in the neutron yield was regularly found when the input energy was slightly increased above a certain level by varying the charging voltage of the capacitor bank. A similar behaviour was found in PF-360 and in PF-1000.

Conclusions

It can be concluded that although during the five decades of PF and Z-pinch research the understanding of the relevant physical processes and technological solutions has reached a high level, there is still a vast field of research ahead. Efficient exchange of knowledge between the various laboratories working in the field, innovative diagnostics and careful evaluation of the results are more important than ever.

A possible way to overcome the presently observed saturation phenomena might be the change and the optimization of the geometry and the material composition of electrodes and insulators, and maybe even also the implementation of gas puffing in the insulator region [19].

References

1. Abd Al-Halim MA (2010) Simulation of Plasma Focus Devices with hemisphere electrodes. J Fusion Energy 29:134–140
2. Bernard A, Coudeville A, Jolas A *et al.* (1975) Experimental studies of the plasma focus and evidence for non-thermal processes. Phys Fluids 18:180–194
3. Filippov NV, Filippova TI, Vinogradov VP (1962) Dense high temperature plasma in the region of non-cylindrical z-pinch compression. Nucl Fusion, Suppl Pt 2:577–587 (in Russian)
4. Herold H, Jerzykiewicz A, Sadowski M *et al.* (1989) Comparative analysis of large plasma focus experiments performed at IPF, Stuttgart, and at IPJ, Świerk. Nucl Fusion 29:1255–1269
5. Jäger U, Herold H (1987) Fast ion kinetics and fusion reaction mechanisms in the plasma focus. Nucl Fusion 27:407–423
6. Jakubowska K, Kubkowska M, Skladnik-Sadowska E *et al.* (2011) Optical emission spectroscopy of plasma streams in PF-1000 experiments. Nukleonika 56;2:125–129
7. Krasa J, Kralık M, Velyhan A *et al.* (2008) Anisotropy of the emission of DD-fusion neutrons caused by the plasma-focus vessel. Plasma Phys Control Fusion 50:125006 (10 p)
8. Kubeš P, Kravárik J, Klir D *et al.* (2009) Determination of deuteron energy distribution from neutron diagnostics in a plasma-focus device. IEEE Trans Plasma Sci 37:83–87
9. Kwiatkowski R, Skladnik-Sadowska E, Malinowski K *et al.* (2011) Measurements of electron and ion beams emitted from the PF-1000 device in the upstream and downstream direction. Nukleonika 56;2:119–123
10. Lee S (1988) A simple facility for the teaching of plasma dynamics and plasma nuclear fusion. Am J Phys 56:62–68
11. Lee S, Saw SH (2008) Neutron scaling laws from numerical experiments. Fusion Energy 27:292–295
12. Lee S, Saw SH, Soto L *et al.* (2009) Numerical experiments on plasma focus neutron yield versus pressure compared with laboratory experiments. Plasma Phys Control Fusion 51:075006 (11 p)
13. Mahmood S, Springham SV, Zhang T *et al.* (2006) Novel fast-neutron activation counter for high repetition rate measurements. Rev Sci Instrum 77:10E713 (4 p)
14. Maisonnier C, Samuelli M, Linhart JG *et al.* (1969) Experiments with imploding plasma liners. In: Proc Plasma Phys Control Nucl Fusion Res, Vol. II, pp 77–86
15. Mather JW (1964) Investigation of the high energy acceleration mode in the coaxial gun. Phys Fluids Suppl:S28–S34
16. Michel L, Schönbach KH, Fischer H (1974) Neutron emission from a small 1-kJ plasma focus. Appl Phys Lett 24:57–59
17. Patou C, Simonnet A, Watteau JP (1968) Dynamique et émission neutronique d'une décharge électrique non cylindrique focalisante. J Phys 29:973–984
18. Schmidt H (1987) The role of beam target processes in extrapolating the plasma focus to reactor conditions. In: Proc of the Workshop PF and Z-pinch Research, 29–30 June 1987, Toledo, Spain, p 65
19. Schmidt H (2001) On the influence of gas puff loads on plasma focus dynamics. Nukleonika 46;1:15–19
20. Schmidt H, Kubeš P, Sadowski MJ *et al.* (2006) Neutron emission characteristics of pinched dense magnetized plasmas. IEEE Trans Plasma Sci 34:2363–2367
21. Schmidt R (1987) Untersuchung über den Ablauf der Fusionsprozesse im Plasmafokus unter Verwendung von zeitaufgelöster Neutronenspektroskopie. PhD dissertation, University of Stuttgart, Stuttgart, Germany
22. Schmidt R, Herold H (1987) A method for time resolved neutron spectroscopy on short pulsed fusion neutron sources. Plasma Phys Control Fusion 29:523–534
23. Scholz M, Karpinski L, Paduch M *et al.* (2010) Development of diagnostics for large-scale experiments in dense magnetized plasmas. In: Proc of the Conf on Plasma Diagnostics, 12–16 April 2010, Pont-à-Mousson, France
24. Velikovich AL, Clark RW, Davis J *et al.* (2007) Z-pinch plasma neutron sources. Phys Plasmas 14:022701 (16 p)